

Critical-current diffraction patterns of grain-boundary Josephson weak links

R. L. Peterson and J. W. Ekin

Electromagnetic Technology Division, National Institute of Standards and Technology, Boulder, Colorado 80303

(Received 7 May 1990)

We discuss the diffraction patterns and other characteristics of the critical current as a function of magnetic field in grain-boundary Josephson barriers. Diffraction patterns occur not just for *SIS* junctions but for all types of Josephson links, including *SNS* junctions, which may be present at grain boundaries in high- T_c superconductors. We discuss the generality of the Airy diffraction pattern, which is expected to characterize grain-boundary barriers in bulk material more accurately than the Fraunhofer pattern. The transport critical-current density in many bulk, granular high- T_c superconductors has a power-law dependence on very low magnetic fields, characteristic of averaged diffraction patterns, and cannot be fitted by an exponential magnetic-field dependence, which may result from the material properties of the barriers.

I. INTRODUCTION

Our modeling studies^{1,2} of critical current density in granular high- T_c superconductors assumed that the principal barriers to transport current at low magnetic field are connected Josephson weak links (JWL), that is, barriers which are characterized by the Josephson $\sin\phi$ relation. The principal fitting parameter in these studies was the average barrier length normal to the applied magnetic field. This scaling length originates in the diffraction patterns common to all such weak links. For a wide variety of samples prepared in several different laboratories, we found that these average lengths were comparable to the grain dimensions. Moreover, they scaled approximately with the grain dimensions in samples having more than an order of magnitude of variation in grain size. These two results suggested that JWL dominate the low-field dependence of the transport critical current in these bulk samples and that the weak links are at the grain boundaries.

Recent experimental work on isolated grain boundaries in thin films has shown current-voltage curves characteristic of resistively shunted Josephson junctions,^{3,4} and (ragged) diffraction patterns,⁵ giving good confirmation for the existence of grain-boundary JWL.

Yet it seems not to be fully appreciated that the critical-current diffraction patterns are characteristic of more than just *SIS'* (superconductor-insulator-superconductor) junctions. Other varieties of JWL, for example *SNS'* (N is normal metal), *SS'S''*, and *SNIS'* junctions, can show diffraction behavior. Many studies of *SNS* junctions have shown Fraunhofer-like patterns, from the early study by Clarke,⁶ to the more recent studies by Paterson⁷ and Hyun *et al.*⁸

Thus one purpose of this paper is to reemphasize the broad foundation for these patterns. We also present a new and more general derivation of the Airy diffraction pattern, and show how it is to be preferred to the Fraunhofer pattern when considering barriers in granular materials. Finally, we relate the results of Hsiang and Finnemore⁹ to the granular materials. These authors pre-

dicted and observed an exponential magnetic field dependence of the critical current in *SNS* junctions with very thick (15–100 μm) and clean normal-metal barriers. Such barriers are not likely to occur in the granular or thin-film high- T_c superconductors.

II. BASIS OF THE DIFFRACTION PATTERNS

The sketch given in this section will be familiar to many, but is presented to emphasize the generality of the diffraction patterns. The derivations of the Josephson $\sin\phi$ equation show its suitability to a wide variety of barriers between superconductors. A good reference to non-tunneling (that is, non-*SIS*) Josephson barriers is that of Likharev.¹⁰ The phenomenological treatment of Barone and Paterno¹¹ generally follows the derivation of Josephson¹² and considers both *SIS'* and *SNS'* junctions. Commenting on all classes of barriers, Likharev has stated,¹³ "Rigorous theory shows that, in most cases, all terms except the first one can be neglected," referring to the most general case

$$J = \sum_{n=1}^{\infty} J_n \sin(n\phi), \quad (1)$$

where J is the supercurrent density and ϕ is the phase difference of the order parameters across the barrier. That is, the simple Josephson equation,

$$J = J_m \sin\phi, \quad (2)$$

applies in most practical cases, including tunnel and non-tunnel sandwiches of any composition, and other types of weak links such as microbridges whose length does not greatly exceed the coherence length of the link material. Even point-contact junctions, the geometry of which make a rigorous theoretical treatment impossible, are very well described by Eq. (2) when the point contact is considered shunted by a resistance, as shown by De Waele and De Bruyn Ouboter¹⁴ and many others.

The material composition and thickness of the barriers determines the magnitude, temperature dependence, and

magnetic field dependence of the maximum current density, J_m . But the mere existence of the barrier, provided that it is thin enough to allow phase coherence across itself, is sufficient to generate the $\sin\phi$ relation together with its generally small distortions, if any.¹⁰ For the existence of this phase relationship, it matters not whether the barrier is a conductor, an insulator, or other material, and the barrier need not be planar. Thus, the magnetic-field dependence contained in $\sin\phi$ applies quite generally to a large class of JWL, not just the SIS structure.

The next piece in the development of the diffraction pattern is the expression for the variation of the Josephson phase difference ϕ along the plane of the barrier. An excellent treatment is given by Van Duzer and Turner.¹⁵ The variation of ϕ is

$$\frac{\Phi_0}{2\pi l} \nabla\phi = \hat{\mathbf{n}} \times \mathbf{B}, \quad (3)$$

where \mathbf{B} is the flux density, from applied and self-fields, in the plane of the barrier, $l = \lambda_r + \lambda_l + t$ is the total field penetration distance, and $\hat{\mathbf{n}}$ is the unit vector normal to the plane of the barrier. If B is constant (in practice this means that the critical current is low enough that the current-generated field is negligible, or equivalently that the barrier dimension is less than about two Josephson penetration lengths), integration of Eq. (3) and substitution into Eq. (2) gives

$$J(x) = J_m \sin(2\pi B l x / \Phi_0 + \phi_0) \quad (4)$$

for \mathbf{B} in the y direction. This is the usual equation from which the diffraction patterns are obtained. If $B = B(x)$, we must use the Maxwell equation $\nabla \times \mathbf{H} = \mathbf{J}$ together with Eqs. (2) and (3) to get a more general equation,^{12,16} which must be solved numerically. In either case, the total current found by integrating the current density over the area of the barrier shows a diffraction pattern as a function of magnetic field.

In the derivation of Eq. (4) or its generalizations, the properties of the barrier are not invoked, except that the barrier must be thin enough that the two superconductors have a coherent-phase relation. Conducting barriers cannot be much thicker than the coherence length in the barrier. Even if the $\sin\phi$ relation is not exact, a diffraction pattern will still result, though not as simple as those obtained from Eq. (4). The basis for the diffraction patterns is thus quite general.

III. THE DIFFRACTION PATTERNS

The shape of the barrier determines the specific form of the diffraction pattern. If the barrier is planar and has the shape of a rectangle of sides L and W , with a constant magnetic field normal to the side of length L , the integration is straightforward. The constant ϕ_0 in Eq. (4) is chosen to maximize the critical current, resulting in

$$I_c(B) = J_m W L \left| \frac{\sin(\pi B / B_0)}{\pi B / B_0} \right|, \quad (5)$$

where

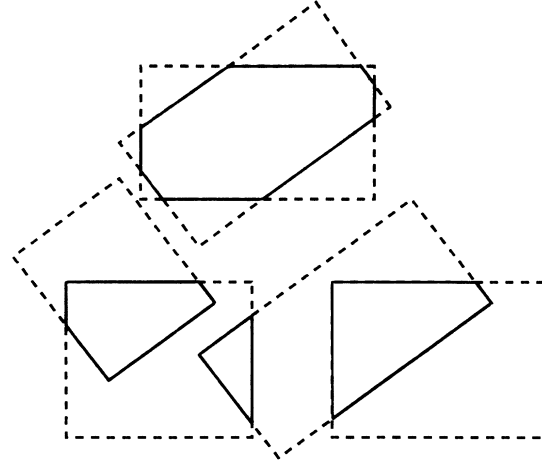


FIG. 1. Illustration of boundary shapes resulting from overlapping rectangles.

$$B_0 = \Phi_0 / (lL). \quad (6)$$

This expression is commonly called the Fraunhofer diffraction pattern, although in optics that term refers to a class of diffraction patterns, not just $|\sin x / x|$. If J_m is not constant, and it may not be for grain-boundary junctions, it must be included in the integration determining I_c ; the Fraunhofer or other type of pattern will then be distorted. Barone *et al.*¹⁷ have studied how random variations in J_m affect the diffraction pattern of a rectangular junction.

In a granular material, the interface between grains will seldom be rectangular, even if the grains have rectangular cross sections. The contact area between two rectangular faces of contacting rectangular parallelepipeds (the basic grain morphology in the current high- T_c superconductors) is generally an irregular polygon having from three to eight sides. Figure 1 illustrates this. In addition, many of the grains in a bulk-sintered sample have irregular shapes in spite of the basic tendency toward platelet growth. Thus a more appropriate barrier shape than rectangular needs to be considered. Further, the magnetic field will not generally be parallel

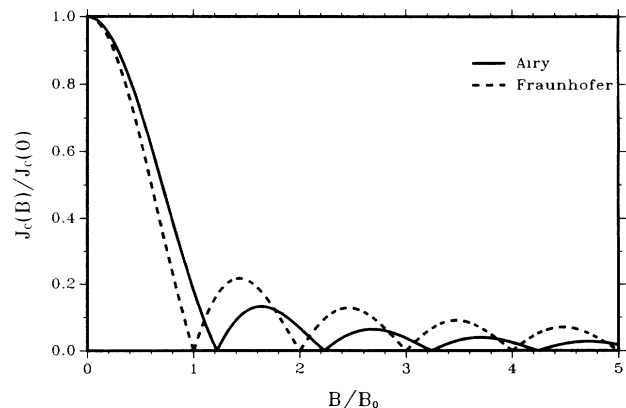


FIG. 2. Comparison of Fraunhofer and Airy diffraction patterns.

to a principal axis of a rectangle or other type of polygon. The Fraunhofer pattern is thus not an adequate basis for the boundaries expected in a granular material.

Barone and Paternò¹¹ show that for a circular planar barrier, the diffraction pattern is of the Airy type

$$I_c(B) = J_m A \left| \frac{J_1(\pi B/B_0)}{\pi B/2B_0} \right|, \quad (7)$$

where A is the area of the barrier and J_1 is the first-order Bessel function. B_0 has the same expression as above, where L is now the diameter of the circle. Figure 2 compares the Fraunhofer and Airy patterns; the principal difference is the field dependence of the envelopes.

But Eq. (7) holds true also for an elliptical barrier, as we now show. The elliptical shape is of particular interest not just because it can be used to simulate the polygonal shape of the contact area between two grains but because Eq. (7) is valid for all orientations of the magnetic field in the plane of the ellipse and is not confined to a principal axis.

Figure 3 shows the geometry. The lengths of the semi-major and semi-minor axes are a and b ; the area A of the ellipse is πab , and its equation is

$$\frac{x^2}{a^2} + \frac{y^2}{b^2} = 1. \quad (8)$$

The applied field is along the direction y' at an angle θ from a principal axis; x' is the dimension to be used in Eq. (4). The current through the barrier is then

$$I = J_m \int_{-a}^a dx \int_{-y_1}^{y_1} dy \sin(kx' + \phi_0), \quad (9)$$

where $y_1 = b(1 - x^2/a^2)^{1/2}$, $k = 2\pi Bl/\Phi_0$, and $x' = x \cos\theta - y \sin\theta$. Before proceeding with the integration, we determine the "length" L of the ellipse as seen by the field B , that is, in the direction normal to the field; this length appears in the result. It is found by calculating the slope dy/dx of the ellipse at the point (x_0, y_0) where the slope is equal to $\cot\theta$. This gives $x_0 = (a^2/S)\cos\theta$ and $y_0 = -(b^2/S)\sin\theta$, where

$$S = (b^2 \cos^2\theta + a^2 \sin^2\theta)^{1/2}. \quad (10)$$

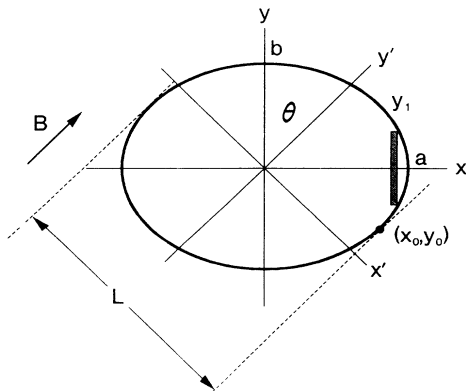


FIG. 3. An elliptical Josephson barrier. A magnetic field lies in the plane of the ellipse at an angle θ from a principal axis.

Because $x'_0 = x_0 \cos\theta - y_0 \sin\theta$, we find $L \equiv 2x'_0 = 2S$.

Integration over y in Eq. (9) and substitution of $x = a \cos\alpha$ gives

$$I = \frac{aJ_m}{k_s} \int_0^\pi d\alpha \sin\alpha [\cos(k_c a \cos\alpha - k_s b \sin\alpha + \phi_0) - \cos(k_c a \cos\alpha + k_s b \sin\alpha + \phi_0)], \quad (11)$$

where $k_s = k \sin\theta$ and $k_c = k \cos\theta$. The simplest way to proceed from here is to use

$$k_c a \cos\alpha \pm k_s b \sin\alpha = kS \sin(\gamma \pm \alpha), \quad (12)$$

where $\tan\gamma = (a/b)\cot\theta$, and S is given in Eq. (10). Then the two cosine terms in Eq. (11) can be expressed as an infinite series of Bessel functions. Only the first-order terms survive the integration on α . Thus

$$I = 2\pi ab J_m \frac{J_1(kS)}{kS} \sin\phi_0. \quad (13)$$

Since

$$kS = \frac{2\pi Bl}{\Phi_0} \frac{L}{2} = \frac{\pi B}{B_0}, \quad (14)$$

Eq. (7) results.

This is a useful result, not so much because many of the polygonal contacts between grains in bulk samples will approximate ellipses, but because it shows that for any orientation of the applied field in the plane of the barrier, the same expression—the Airy pattern—may be used as the starting point in an averaging process in granular materials. The field orientation appears only in L , the projection of the ellipse normal to the field.

The field dependence of the envelope of the Airy pattern at large B is $B^{-3/2}$, as contrasted with the B^{-1} of the Fraunhofer pattern when B is along a principal axis. But this falloff is by no means the most rapid of the possible diffraction patterns. When the field is along the principal axis of a lens-shaped barrier, the pattern generally falls off yet more steeply,¹⁸ and is sensitive to the details of the shape. Thus we expect that in a bulk granular material, the averaged diffraction pattern will have an exponent in a power-law field dependence of about $-\frac{3}{2}$ or a little greater in magnitude.

IV. FIELD DEPENDENCE OF A JOSEPHSON WEAK-LINK NETWORK

Every percolation path in a network of Josephson barriers has a weakest link that will control J_c for that path. Cross linking these percolation paths still results in the weakest links controlling the network J_c . Our modeling and fitting studies^{1,2} showed that the planes of these weakest links must be within a few tens of degrees from the direction of the applied field, as would be expected. The field dependence of these weakest links, which will have a distribution of areas, then characterizes $J_c(B)$ for the network of barriers. Area and field-angle averages of the basic diffraction patterns showed that at $B > B_0$, the field dependence of the critical current density based on

the Airy pattern varies as $B^{-3/2}$ whereas that based on the Fraunhofer pattern varies as B^{-1} , consistent with their envelopes. The difference is significant; the former is found to fit the $J_c(B)$ dependence of a wide range of bulk sintered superconductors much better than the latter.²

For thick SNS junctions, the factor J_m has been shown⁹ to vary as $\exp(-K_N d_N)$, where d_N is the thickness of the normal metal barrier and K_N^{-1} is the decay length of the order parameter in the normal metal. For SNS barriers which are not thick, and for the SNS-type barriers which may exist at grain boundaries, the thickness dependence of J_m is less certain.¹⁰ Hsiang and Finemore⁹ have made an often-referenced calculation for an SNS junction in which the normal-metal barrier was very thick (much greater than the decay length of the order parameter in the normal metal), and "clean" (electron mean free path much greater than the coherence length). They argued that K_N should vary approximately as the applied field in this case, and indeed observed an approximate exponential dependence of J_m on field in such junctions, in which the thickness of the normal-metal barrier ranged from 15μ to $100 \mu\text{m}$. It is noteworthy that Clarke,⁶ Paterson,⁷ and Hyun *et al.*⁸ saw only the diffraction pattern in their SNS junctions that had normal-metal barriers well under $1 \mu\text{m}$ thick.

Since $K_N d_N \approx B/B_N$ according to Hsiang and Finemore⁹ (HF), the characteristic field of the exponential

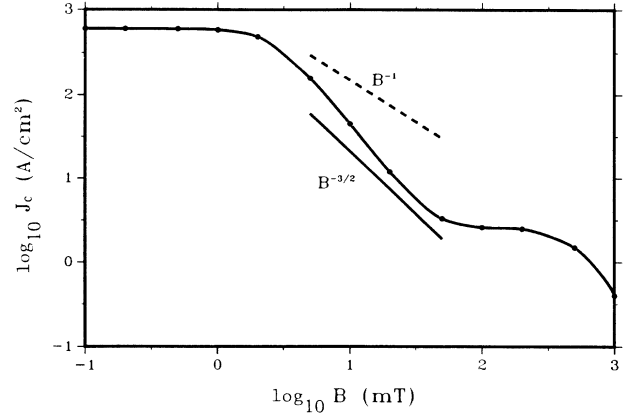


FIG. 5. Critical current density of another granular sample of Y-Ba-Cu-O, plotted on a log-log scale, showing J_c over a large range of magnetic field. Two straight lines showing B^{-1} and $B^{-3/2}$ are also shown.

variation B_N would vary inversely with the barrier thickness d_N . To a good approximation it also depends only on the properties of the normal metal, and not the adjacent superconductors.⁹ The "decoupling" field B_0 of the diffraction pattern for their thick junctions would have been of the order of $1 \mu\text{T}$, as they pointed out, whereas their B_N was of the order of 1mT . Since grain-boundary weak links in high- T_c superconductors should have

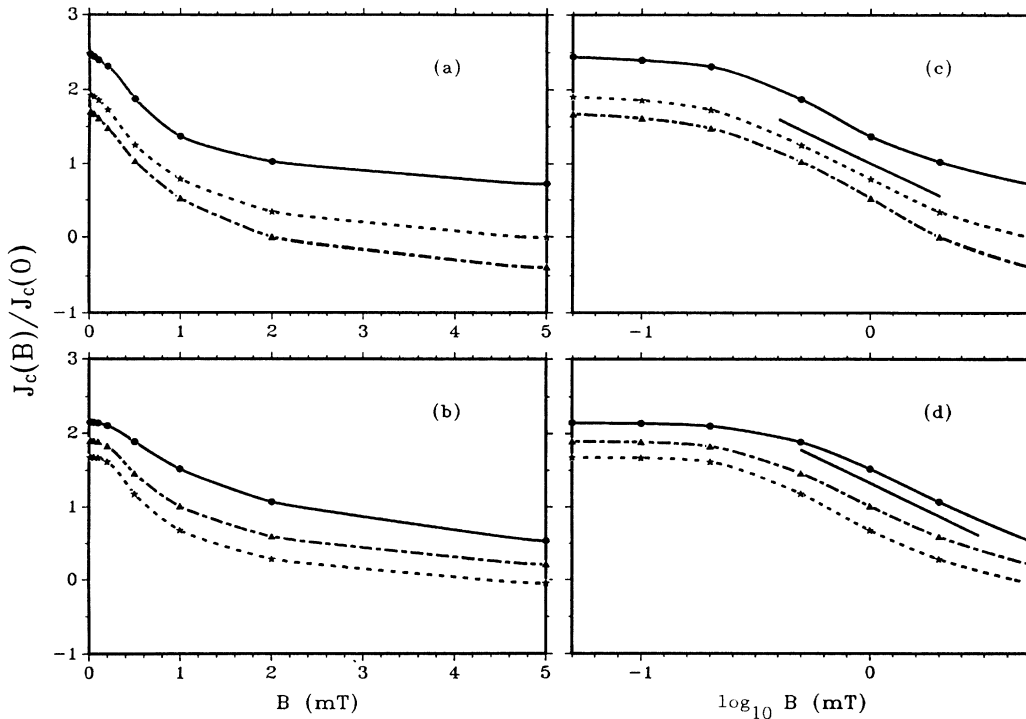


FIG. 4. (a) and (b) log-linear plots of J_c vs B measurements on six different granular samples, showing no linear regions, that is, regions in which the current is exponential in B . (c) and (d) log-log plots for the same samples, plotted over the same field range; the data in (c) are those of (a); the data in (d) are those of (b). The three samples of (a) and (c) have decoupling fields B_0 [see Eq. (10)] of 0.3 – 0.4mT . The three samples of (a) and (d) have decoupling fields of 0.5 – 0.7mT . The straight solid lines of (c) and (d) are drawn with slopes of $-3/2$ to show that the data vary approximately as $B^{-3/2}$ for $B > B_0$.

thicknesses of one to a few tens of nanometers, the thicknesses which HF considered are 3 to 4 orders of magnitude greater than expected in granular samples. Thus unless the material properties of the junctions at the boundaries in a granular sample are quite unusual, SNS barriers there would be far too thin to see an exponential field dependence at the low fields B_0 where decoupling is observed, even if the HF analysis applied. The characteristic field B_N of the exponential decay in the granular samples should be of the order of 1 T, which is orders of magnitude greater than the observed low-field drop in J_c that occurs in the 0.1–10 mT range. Still, we should mention that England *et al.*¹⁹ observed an exponential decay of J_c with a B_N on the order of 1 T in single-grained epitaxial thin films of $\text{YBa}_2\text{Cu}_3\text{O}_x$ (Y-Ba-Cu-O). In order to make connection with the HF theory, they postulated the existence of microscopic SNS defects within the films, even though the measured temperature dependence of J_c did not agree with SNS theory.

The shapes of the $J_c(B)$ curves in granular high- T_c superconductors fit a power-law dependence at low fields. We have plotted in Fig. 4 the transport critical current data taken previously² on six different bulk granular samples to see whether they could be fitted with an exponential magnetic-field dependence. As is seen in Figs. 4(a) and 4(b), the data do not follow such a form in the decoupling regime. Instead they conform well to a $B^{-3/2}$ power law, as seen in Figs. 4(c) and 4(d), before leveling off at higher fields. In Fig. 5 we show the measured transport critical current in a different sample of Y-Ba-Cu-O through the whole magnetic-field range up to 1 T. It too shows the power-law decrease over almost 3 orders of magnitude of J_c in the range of the decoupling field. The decrease observed is slightly steeper than $B^{-3/2}$ and may be due to the influence of some lenticular shaped

boundary interfaces,¹⁸ as discussed earlier. At larger fields (0.1 T) a nearly field-independent percolation current through non-Josephson connections takes over before the final drop at about 1 T signifying the approach to B_{c2} .

V. SUMMARY AND CONCLUSIONS

The magnetic-field dependence of the critical current through JWL enters in two ways. First, it comes from the quantum interference effect common to all Josephson barriers, including SIS' , SNS' , $SS'S''$, and $SNIS'$ junctions. If the barrier is not precisely described by a $\sin\phi$ relation, a diffraction pattern will still result but will not be as simple as those described above. The specific form of the critical-current pattern depends on the shape of the barrier. We have shown here that for the interfaces expected in the granular high- T_c superconductors, the pattern should be closer to the Airy type than to the Fraunhofer type, and we have shown the calculation leading to the Airy pattern for elliptical barrier shapes.

Second, the magnetic field can make itself felt through the properties of the parameters which go into the expression for the maximum critical current. The analysis of Hsiang and Finnemore⁹ for clean, thick SNS junctions would not seem to apply to the thin grain-boundary junctions characterizing high- T_c superconductors; if it does, its predicted exponential decay constant would likely be of the order of 1 T. Further, an exponential magnetic-field dependence does not fit the low-field (≤ 10 mT) decrease of $J_c(B)$ in the samples we have measured.

The field characteristic obtained from the averaged Airy diffraction pattern is consistent with the observed $J_c(B)$ curves in granular high- T_c superconductors, both in the magnitude of the decoupling field as well as in the power-law dependence.

¹R. L. Peterson and J. W. Ekin, Phys. Rev. B **37**, 9848 (1988).

²R. L. Peterson and J. W. Ekin, Physica C **157**, 325 (1989).

³D. Dimos, P. Chaudhari, and J. Mannhart, Phys. Rev. B **41**, 4038 (1990).

⁴B. H. Moeckly, D. K. Lathrop, G. F. Redinbo, S. E. Russek, and R. A. Burhman (unpublished).

⁵S. E. Russek and R. A. Burhman, *Proceedings of the Conference on the Science and Technology of Thin-Film Superconductors, Denver, 1990* (Plenum, New York, in press).

⁶J. Clark, Proc. R. Soc. A **308**, 447 (1969).

⁷J. L. Paterson, J. Low Temp. Phys. **35**, 371 (1979).

⁸O. B. Hyun, J. R. Clem, and D. K. Finnemore, Phys. Rev. B **40**, 175 (1989).

⁹T. Y. Hsiang and D. K. Finnemore, Phys. Rev. B **22**, 154 (1980).

¹⁰K. K. Likharev, Rev. Mod. Phys. **51**, 101 (1979).

¹¹A. Barone and G. Paternò, *Physics and Applications of the Josephson Effect* (Wiley, New York, 1982), Chap. 1.

¹²B. D. Josephson, Adv. Phys. **14**, 419 (1965).

¹³K. K. Likharev, *Dynamics of Josephson Junctions and Circuits* (Gordon and Breach, New York, 1986), p. 7.

¹⁴A. Th. A. M. De Waele and R. De Bruyn Ouboter, Physica **41**, 225 (1969).

¹⁵T. Van Duzer and C. W. Turner, *Principles of Superconductive Devices and Circuits* (Elsevier, New York, 1981), Section 4.03.

¹⁶C. S. Owen and D. J. Scalapino, Phys. Rev. **164**, 538 (1967).

¹⁷A. Barone, G. Paternò, M. Russo, and R. Vaglio, Zh. Eksp. Teor. Fiz. **74**, 1483 (1978) [Sov. Phys.—JETP **47**, 776 (1978)].

¹⁸R. L. Peterson, Cryogenics (to be published).

¹⁹P. England, T. Venkatesan, X. D. Wu, A. Inam, M. S. Hegde, T. L. Cheeks, and H. G. Craighead, Appl. Phys. Lett. **53**, 2336 (1988).

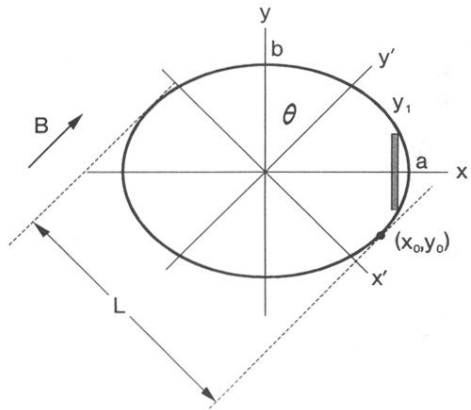


FIG. 3. An elliptical Josephson barrier. A magnetic field lies in the plane of the ellipse at an angle θ from a principal axis.